CHEMISTRY JOURNAL OF MOLDOVA. General, Industrial and Ecological Chemistry. 2021, 16(2), 102-111
ISSN (p) 1857-1727 ISSN (e) 2345-1688
http://cjm.asm.md
http://dx.doi.org/10.19261/cjm.2021.911

V_2O_5 NANOPARTICLES FOR DYES REMOVAL FROM WATER

Thamer Adnan Abdullah [a,b], Tatjana Juzsakova [a], Rashed Taleb Rasheed [b], Ali Dawood Salman [a], Mohammademad Adelikhah [c], Le Phuoc Cuong [d], Igor Cretescu [e*]

[a]*Sustainability Solutions Research Lab, Bio-, Environmental and Chemical Engineering Research and Development Center, Faculty of Engineering, University of Pannonia, 10, Egyetem str., Veszprem 8200, Hungary*
[b]*Chemistry Branch, Applied Sciences Department, University of Technology, Baghdad 19006, Iraq*
[c]*Institute of Radiochemistry and Radioecology, University of Pannonia, 10, Egyetem str., Veszprém 8200, Hungary*
[d]*University of Danang-University of Science and Technology, 54, Nguyen Luong Bang str., Danang 550000, Vietnam*
[e]*Faculty Chemical Engineering and Environmental Protection, "Gheorghe Asachi" Technical University of Iasi, 73, D. Mangeron blvd., Iasi 700050, Romania*
[*]*e-mail: icre1@yahoo.co.uk; icre@tuiasi.ro; phone: (+40) 741 914 342*

Abstract. Rapid population growth, urbanization and industrialization pose significant threats to the aquatic ecosystem. The discharge of untreated dyes contaminated wastewater causes harmful chemical and biological changes in water bodies as well as human disease. The most common dye used at industrial scale is methylene blue (MB). Recently, numerous metal oxide nanoparticles adsorbents have been applied for the purpose of treatment of water from dyes. This paper deals with V_2O_5 nanoparticles adsorbents, obtained by thermal pre-treatment carried out by increasing the temperatures between 90 and 750°C. The surface chemistry of the newly prepared nanoparticles was investigated by X-ray diffraction and scanning electron microscopy, Fourier Transform infrared spectroscopy and thermogravimetric techniques. Furthermore, the prepared nanoparticles were tested for MB removal from modelled water solution. The obtained results indicated that high MB removal efficiency (93%) and adsorption capacity (27 mg/g) after 40 min of adsorption were obtained for samples of V_2O_5 annealed at 500ºC in comparison with V_2O_5 treated at 90, 250 and 750ºC, respectively. The applicability and suitability of the two kinetic models were tested and the removal mechanism was proposed.

Keywords: hydrothermal method, annealed vanadium pentoxide, methylene blue adsorption, nanoparticle.

Received: 04 November 2021/ Revised final: 12 December 2021/ Accepted: 16 December 2021

Introduction

The intensive development of agricultural, pharmaceutical, and chemical industry has resulted in the release of diverse chemical compounds such as antibiotics, pesticides, plastics,and dyes into an aquatic environment [1]. These industries serve as ideal contributors towards the contamination of aquatic environment since manifold chemicals are discharged directly and very frequently into the environment [2]. As a result, discharging dyes into the aquatic environment affects the water with undesirable colour and toxicity [3]. Consequently, the phenomenon of photosynthesis for aquatic plants is affected as the presence of dyes hinders the penetration or transmission of sunlight [4]. Most of dyes are stable towards light and therefore remain non-biodegradable. Methylene blue (MB) is categorized as a cationic dye, which is also a widely used dyestuff at industrial scale [5,6]. The long-term accumulation of dyes leads to serious threats not only to humans but also aquatic species majorly causing homeostasis and genetic mutation [7]. Removal of hazardous substances such as dyes from aqueous environment has attracted wide attention of researchers to ensure the safety of waterways in particular and environment in general. In order to make the aquatic environment dye-free, various biological, physical, and chemical methods have been reported extensively, which includes adsorption [8,9], membrane filtration [10-12], ozonation [13-15], oxidation [16,17], electro-coagulation [18,19] and biosorption [20,21]. However, it is well established that single treatment is not enough to carry out complete removal of complex compounds such as dyes. Hybrid methods have also been devised and successfully applied for complete MB removal or decomposition from industrial effluents. Consequently, advanced sorbent materials have made adsorption techniques to be economical and more effective since the materials are affordable, efficient and cost-competitive for the MB depollution control

from industrial wastewaters [22]. The transition metals oxide nanoparticles such as CuO, Fe_2O_3, ZnO, MnO_2 and V_2O_5 have been widely used as photocatalysts for water purification [23-26]. These photocatalytic materials exhibit larger surface area, chemical stability, and efficient recyclability while yielding no secondary pollutants [27]. V_2O_5 nanoparticles have been applied in numerous photocatalytic degradation applications because of their non-toxic properties, narrow band gap (~2.4-2.8 eV), better chemical and electrical stability. In order to overcome the limitations of V_2O_5 nanoparticles, their morphology needs to be modified. Carbon nanotubes (CNTs) are the best choice to be combined for the efficient and effective use of V_2O_5 nanoparticles for dyes removal. V_2O_5 nanostructured materials can be in the form of nanoparticles, nanowires, nanorods, nanobelts, nanoribbons, and nanosheets in desired size and morphology with their distinct geometry and new physical and chemical properties [24]. To reduce the poor mechanical strength of metal oxide nanomaterials, nanocomposites are increasingly used for purification of wastewater for removing unwanted species [22,28]. The combination of nano-adsorbent with metal oxide nanoparticles has been the first choice for researchers as adsorbent material. In recent years, researches have been done all over the world to prepare and characterize the nano-size metal oxides [14,17,27,29,30]. The use of nanometal oxides as adsorbents is a promising technique in cleaning water for major water pollutants such as heavy metals, aromatic compounds and dyes [27,28].

The aim of this work was set to prepare and investigate the V_2O_5 nanoparticles for the methylene blue removal from aqueous solutions. Additionally, the effect of heat treatment on V_2O_5 nanoparticles produced by the hydrothermal method was investigated. The physico-chemical characteristics of the obtained V_2O_5 nanoparticles were correlated with their sorption properties. Moreover, the kinetic data were analyzed using the pseudo-first and pseudo-second order rate equations.

Experimental

Materials

Ammonium-metavanadate (99.99%), nitric acid (99%), cetyltrimethylammonium bromide (CTAB99%) and ethanol (99.8%) were purchased from Merck (Budapest, Hungary).

Synthesis of V_2O_5 nanoparticles

V_2O_5 nanoparticles were prepared by the hydrothermal method. For this process, ammonium metavanadate (0.1 g) and CTAB (0.1 g) were dissolved in 100 mL water-ethanol solution with a ratio of 7:3, respectively. This was followed by the dropwise addition of nitric acid whilst continuously being stirred until the acidic pH 2.5 was achieved. The mixture above was heated under reflux for 6 h at 80°C. The orange precipitate was isolated and washed with distilled water (10 times) and ethanol. Then it was dried in oven at 90ºC for about 1 h. The mixture was annealed for 2 h at relevant temperatures of 250, 500 and 750°C, respectively. Eq.(1) represents the formation of vanadium hydroxide during the preparation step [31].

$$2NH_4VO_3 + 2HNO_3 + nH_2O \xrightarrow{Ethanol/CTAB} V_2O_5nH_2O + 2NH_4NO_3 + H_2O \quad (1)$$

Characterization of prepared samples

The *XRD study* was carried out on a Lab X-6000 Instrument SHIMADZU (Japan), equipped with Cu-Kα radiation (λ= 0.1541 nm).

The morphology of the nanoparticle surface was investigated by *scanning electron microscopy* (SEM) on an Instrument TESCAN Mira3 (Czech Republic).

Fourier Transform infrared spectroscopic (FTIR) measurements were carried out by using a Perkin Elmer Company (USA) spectrometer on grinded samples without additional sample manipulation, in the range of 400 and 4000 cm^{-1}, at a resolution of 2 cm^{-1}, at room temperature.

UV-Vis spectroscopy measurements were done on an UV-Vis Nanocolor spectrophotometer, Macherey-Nagel (Germany).

Thermogravimetric measurements (TG/DTG/DTA) were carried out using a Derivatograph-C type thermobalance (Hungarian Optical Works, Budapest). Samples were measured in ceramic crucibles. The curves were registered while heating the samples to 850°C (at 5°C/min heating rate) in static air atmosphere.

Determination of methylene blue

The maximum absorbance of MB solution in water at a concentration of 20 mg/L was monitored by UV-Vis spectroscopy in the range of 400 to 700 nm. The maximum absorbance (λmax) was observed at 665 nm. The stock solution was used to prepare calibration solutions for with different MB concentrations (4, 8, 12 16, 18 and 20 mg/L) as reported previously [32].

Methylene blue adsorption experiments

The MB removal experiments were accomplished in batch mode as previously reported [32]. MB stock solutions were diluted with distilled water. The pH of the dye solution was set to the desired pH= 7, using 0.1 N NaOH or 0.1 N HCl. For each experiment, 20 mg of

V_2O_5 nanoparticles were added to the 30 mL solution of MB (20 mg/L). The MB removal efficiency was studied as a function of contact time, adsorbent dosage and also the temperature in order to figure out the beneficial conditions for MB removal from water. After the reaction was complete, the samples were stockpiled and taken for separation. The dye concentration in the supernatant was checked using the UV-Vis spectrometer at 665 nm. The percentage MB elimination/removal (RE, %) was calculated by using Eq.(2) [33,34].

$$RE = \left(\frac{C_0 - C_t}{C_0}\right) \cdot 100\ \% \qquad (2)$$

where, C_o denotes the initial MB concentration (mg/L);
C_t represents the MB concentration at time t (mg/L).

The adsorbed amount of MB (q_t) was calculated using Eq.(3) [33,34].

$$q_t = \frac{(C_\circ - C_t)}{m} \cdot V \qquad (3)$$

where, V stands for volume of solution (L);
m denotes the weight of prepared metal oxides (g);
q_t is adsorption capacity of MB at time t (mg/g).

Each experiment was performed in triplicate under identical conditions and the mean values were calculated and reported in this work.

Results and discussion

Characterisation of V_2O_5 nanoparticles

The surface morphology of the obtained V_2O_5 nanoparticles was investigated by using Fourier Transform infrared spectroscopy, X-ray diffraction, SEM, and thermogravimetric analysis. The FTIR spectra of V_2O_5 as prepared and annealed samples are shown in Figure 1. The broad and weak band at 3500 cm^{-1} and a peak at 1661 cm^{-1} can be assigned to the O-H stretching and H-O-H bending vibrations respectively, which indicate the existence of coordinated water molecules. The band at 3217 cm^{-1} corresponds to the asymmetric stretching vibration of ammonia [35] originated from starting material of NH_4VO_5. Bands mentioned above disappeared after treatment at higher annealing temperatures. The main peaks are at 1027, 831 and 610 cm^{-1} on all spectra, which can be assigned to V=O stretching, V-O-V asymmetric and V-O-V bonds symmetric vibrations [36,37].

The XRD technique was used to investigate the crystallinity of the newly prepared nanomaterials. Figure 2 represents the XRD patterns of V_2O_5 nanomaterials which were treated at increasing temperatures of 90, 250, 500 and 750°C respectively. The major diffraction peaks of V_2O_5 appear at 2θ= 15.62°, 20.04°, 21.80°, 31.4° and 40.9°, which correspond to (200), (010), (101), (301) and (002) reflections, respectively [27,28]. These peaks relate to the shcherbinaite orthorhombic crystalline structure of V_2O_5 (JCPDS Card No. 41-1426) [31]. With increasing the pre-treatment temperature from 250 to 750°C, the intensity of diffraction peaks increased. Based on the Scherrer's calculation, the mean size of treated V_2O_5 nanomaterials was calculated to be approximately 20 nm. The UV-Vis study also showed structural modification during vanadium metal oxide phase change from amorphous to crystalline. During the calcination process from 90 to 750°C, the energy gap increased from 2.55 to 2.76 eV respectively, and the so-called Bursteine-Moss effect can be observed [31,38].

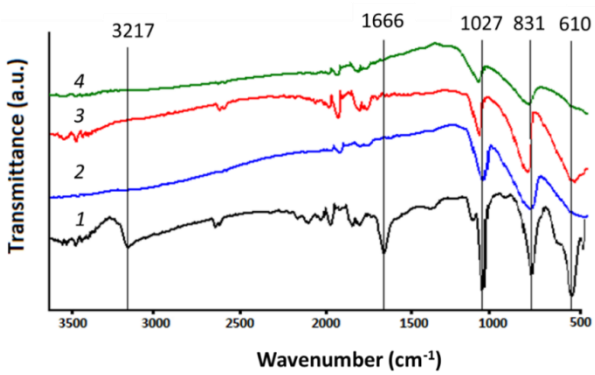

Figure 1. FTIR spectra of theV_2O_5 samples dried at 90°C and annealed at 250, 500 and 750°C temperatures: *1*- V_2O_5 as prepared; *2*- V_2O_5 treated at 250°C; *3*- V_2O_5 treated at 500°C; *4*- V_2O_5 treated at 750°C [31].

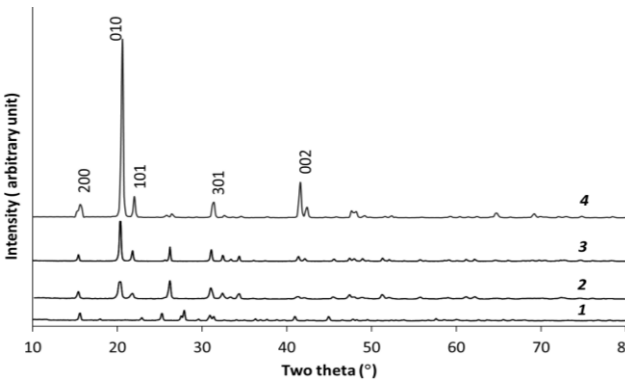

Figure 2. XRD patterns of theV_2O_5 nanoparticles treated at different temperatures: *1* - V_2O_5 as prepared; *2* - V_2O_5 treated at 250°C; *3* - V_2O_5 treated at 500°C; *4* - V_2O_5 treated at 750°C.

The SEM images of the V_2O_5 nanoparticles pre-treated at 500°C are shown in Figure 3, indicating that V_2O_5 particles appeared in the form of nanoflakes [31].

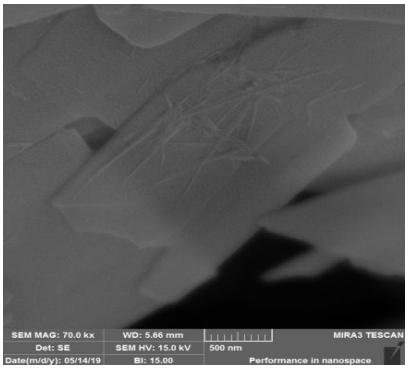

(a)

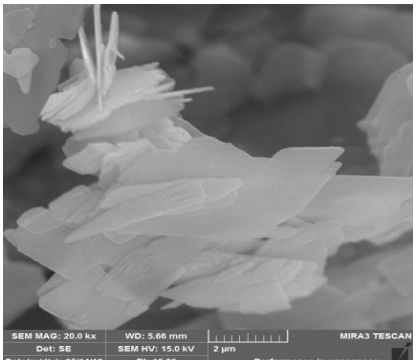

(b)

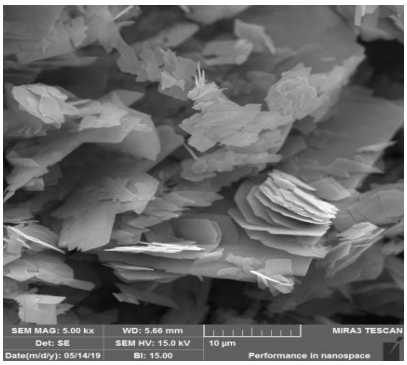

(c)

Figure 3. SEM images of V_2O_5 nanoparticles annealed at 500°C, at a resolution of 500 nm *(a)*; 1 µm *(b)*; 10 µm *(c)*.

Furthermore, the obtained V_2O_5 nanoparticles were studied by thermogravimetric methods in a temperature range from 23 to 850°C with a heating rate of 5°C/min. The sample studied showed mainly amorphous structure with some $(NH_4)_2V_6O_{16}$ crystalline phase as confirmed by XRD analysis. Sample weight at the beginning of the analysis was 62.2 mg. The decomposition curves of V_2O_5 nanoparticles are given in Figure 4, and the mass loss data are given in Table 1. According to the obtained results on V_2O_5 nanoparticles, the TGA and DTG curves indicated five stages from room temperature up to 850°C [31,39-41].

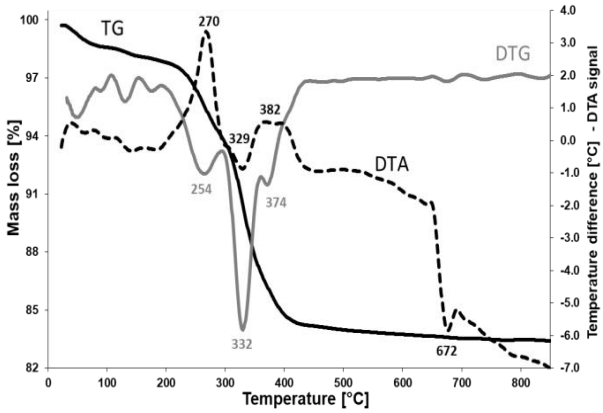

Figure 4. Thermogravimetric curves (TG/DTG/DTA) of V_2O_5.

Evaluation of V_2O_5 nanoparticles efficiency in methylene blue removal

The study was carried out on V_2O_5 nanoparticles as prepared and pre-treated at 250, 500 and 750°C with contact time from 0 to 50 min. The UV-Vis measurements were done every 10 min. The initial MB concentration, MB solution volume and weight of samples were as follows: 20 mg/L, 30 mL and 20 mg, respectively. The results are summarized in Figures 5 and 6 as well as Table 2, showing that MB concentration reached the lowest concentration after adsorption experiment using V_2O_5 nanomaterials treated at 500°C in comparison to the other samples.

Table 1

Mass loss data from the thermogravimetric measurements.

Stage	*$T_{initial}$ (°C)*	*T_{final} (°C)*	*T_{max} (°C)*	*Mass loss (m%)*	*Mass loss due to*
1	23	200	-	1.9	dehydration
2	200	293	254	3.9	removal/oxidation of compounds used during preparation
3	293	355	332	6.6	decomposition of $(NH_4)_2V_6O_{16}$ to V_2O_5
4	355	450	374	3.2	beginning of crystallization
5	450	-	850	0.8	crystallization step and/or decomposition of bulk impurities
Sample mass: 62.2 mg					**Total mass loss: 16.40%**

Hence, removal efficiency as well as the adsorption capacity values were higher for V_2O_5 nanoparticles annealed at 500°C as shown in Figure 6 and Table 2. It should be noted that the increase in the MB removal efficiency over the studied samples was significant up to 40 min, after which was slowly decreased for the following 10 min.

Table 2

MB removal efficiency and adsorption capacity of V_2O_5 nanoparticles at 40 min of contact time.

Adsorbents	*RE (%)*	*q_t (mg/g)*
V_2O_5 as prepared	49.1	15.1
V_2O_5 at 250°C	52.4	16.0
V_2O_5 at 500°C	93.1	27.2
V_2O_5 at 750°C	65.1	19.8

Following this, the adsorption experiment was studied in dosage range between 15 mg and 90 mg, at room temperature (RT) (Figure 7). Thus, the sample of 60 mg of V_2O_5 nanoparticles annealed at 500°C presented the highest MB uptake from water at the following parameters: T= 40 min, C_{MB}= 20 mg/L, V= 30 mL, T= RT (Figure 7). It was noted that when the temperature increased the MB removal was increased, and the optimum solution temperature presented higher removal efficiency at 45°C (Figure 8).

The comparison of sorption capacity of the V_2O_5 nanoparticles to other commercially available sorption materials (Table 3) indicated that the obtained V_2O_5 nanoparticles exhibited improved sorption properties for MB.

Table 3

Comparison of various sorption capacities of different adsorbent materials reported for MB removal from water samples.

Adsorbents	*Adsorption capacity mg/g*	*Reference*
MgO	4.5	[42]
Fe_2O_3 modified MWCNTs	42.0	[43]
Red mud waste	4.1	[44]
Ceria nanofibers	10.0	[45]
Ceria nanoparticles	18.0	[46]
HCl treated fly ash	8.0	[47]
Animal waste ash	5.2	[48]
Clay nanoparticles	6.3	[49]
Co-Fe_2O_3 modified MWCNTs	14.3	[50]
Zeolite	10.9	[51]
Fe_3O_4 modified graphene	33.7	[52]
Polyaniline nanotube	4.8	[53]
Brown peat	24.3	[54]
Fe_3O_4 chitosan composite	45.1	[55]
NaOH treated fly ash	10.2	[56]
ZnO nanoparticles	9.6	[57]
V_2O_5 nanoparticles	***27.2***	***This work***

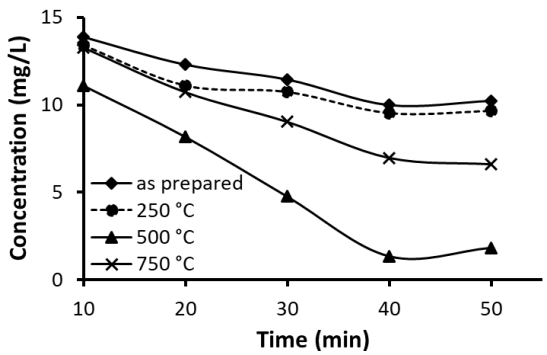

Figure 5. Change in MB concentration against time over V_2O_5 nanoparticles as prepared and annealed at different temperatures.

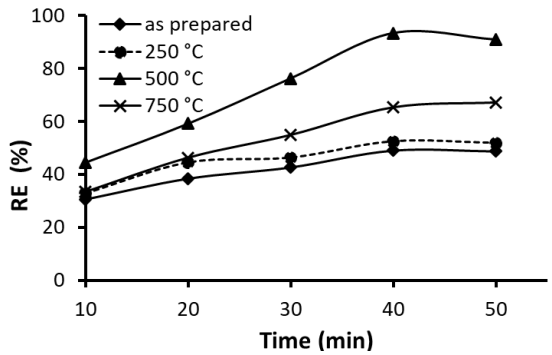

Figure 6. Removal efficiency (RE %) of MB from water against time over V_2O_5 as prepared and annealed at different temperatures.

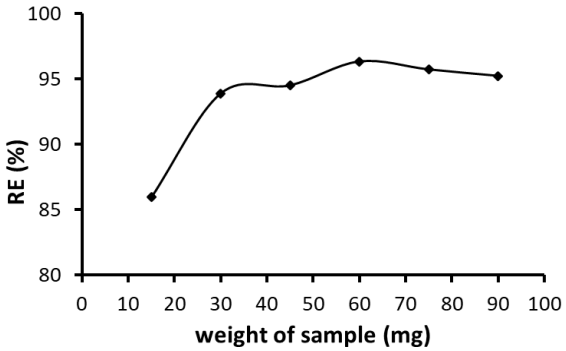

Figure 7. Effect of adsorbent dosage on MB removal over V_2O_5 nanoparticles annealed at 500°C.

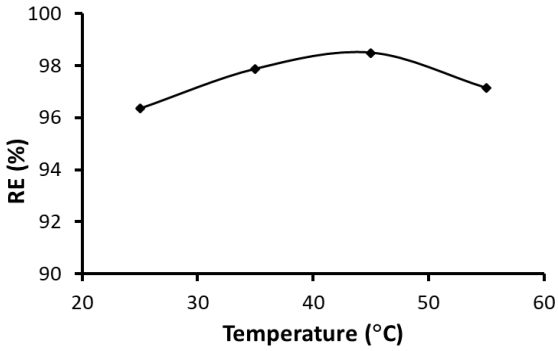

Figure 8. Effect of solution temperature on MB removal over V_2O_5 nanoparticles annealed at 500°C.

Kinetic studies

The kinetic models are relatively efficient for the determination of the rate at which adsorbent efficiently removed the adsorbate such as pollutants including non-biodegradable dyes from wastewater [58]. The data analysis reveals that the highest adsorption as well as the best removal was achieved using V_2O_5 nanoparticles was at annealing temperature of 500°C. In order to find out the rate of removal of MB dye from wastewater, the obtained experimental data for MB adsorption study was analysed using pseudo-first and pseudo-second order kinetic models [59]. Figures 9 and 10 show the resulting graphs from two kinetic models for MB adsorption. Figure 9 presents the pseudo-first order kinetic model with R^2 value of 0.967.

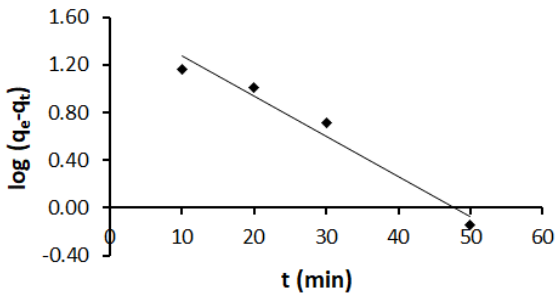

Figure 9. Pseudo-first order plot for MB adsorption onto V_2O_5 annealed at 500°C, where *y= -0.0336x + 1.6087* is linear form of plot and R^2= 0.9672 denotes the linear regression value.

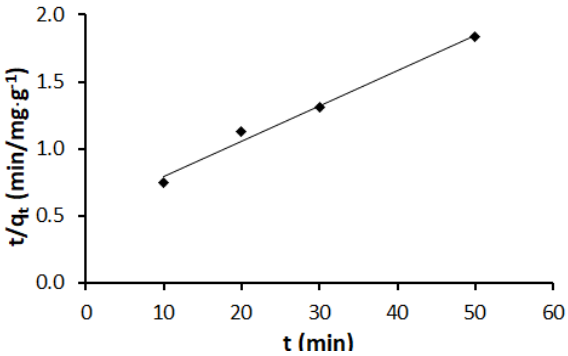

Figure 10. Pseudo-second order plot for MB adsorption onto V_2O_5 annealed at 500°C, where *y= -0.0263x + 0.533* is linear form of plot and R^2= 0.9882 denotes the linear regression value.

The statistical analysis of the adsorption data confirmed that pseudo-second order is the most suitable kinetic model at the lower solute concentration [60]. Similar to literature data, the plot confirmed that pseudo-second order is the best fitting model to interpret and depict the MB adsorption procedure having the high correlation coefficient (R^2) value of 0.988 (Figure 10). It exhibited linear regression between the adsorbent and removal of MB dye from wastewater as previously reported by Somsesta, N. *et al.* [61], Tuli, F.J. *et al.* [62] and Tran, T.H. *et al.* [63] on various adsorbent materials.

The sorption mechanism of MB into V_2O_5 nanoparticles can be understood in the following way: ionic bond forms between the negatively charged oxygen atom on the metal-oxide nanoparticles and the positively charged sulphur in methylene blue, and bond can form on the opposite side of vanadium as shown in Figure 11.

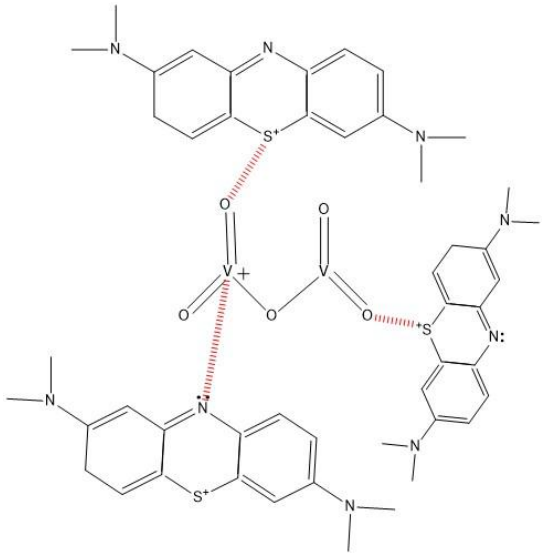

Figure 11. Proposed adsorption mechanism between MB and V_2O_5 nanoparticles.

Conclusions

The vanadium oxides nanoparticles were successfully synthesized *via* hydrothermal method and treated at different temperatures (90, 250, 500 and 750°C). The nanostructure of prepared material was confirmed by FTIR, X-ray diffraction and SEM study.

It was confirmed by FTIR spectroscopy that the surface dehydroxylation and decomposition of the starting material NH_4VO_5 occurred at 250°C. Similar observation was made by TG study, which showed that the thermal decomposition of NH_4VO_5 to V_2O_5 occurs between 293 and 355°C. The XRD data showed that the orthorhombic crystalline structure of V_2O_5 begins to form at an even lower temperature of 90°C, and well-defined crystalline structures was observed at 750°C. The heat treatment leads to a significant increase in the crystallinity of samples but at the same time can cause a decrease in sample surface area. The reduction of sample adsorption area can explain the decrease in the sorption activity

sample annealed at 750°C towards the removal of the methylene blue.

On the other hand, the obtained results indicated that the heat-treated vanadium samples at temperature ranging between 90 and 750°C have rather high adsorption capacity, varying from 15 to 27 mg/g, towards MB removal from water in comparison with other sorbents reported (4-45 mg/g). It was found that an increase in the adsorbent dose up to 60 mg and slight increase in the temperature of solution (*V*= 30 mL) from RT to 45°C leads to the maximum removal efficiency, 98%, of MB (20 mg/L) from water after 40 min of treatment. The applicability and suitability of two common kinetic models was tested. These results demonstrated that the best fit of experimental adsorption data was to the pseudo-second order model.

The presented work showed that V_2O_5 nanoparticles could find a practical application for the removal of organic industrial pollutants from wastewater such as methylene blue dye.

Acknowledgments

The authors would like to thank to the University of Technology, Baghdad, Iraq, for tests and measurements and to the Hungarian GINOP-2.2.1-15-2017-00106 project: Complex utilization of red mud and recovery of rare earth metals from red mud, from Pannonia University, Veszprém, Hungary.

Funding

This work was supported by the GINOP-2.2.1-15-2017-00106 project: Complex utilization of red mud and recovery of rare earth metals from red mud, Veszprém, Hungary.

References

1. Tkaczyk, A.; Mitrowska, K.; Posyniak, A. Synthetic organic dyes as contaminants of the aquatic environment and their implications for ecosystems: A review. Science of The Total Environment, 2020, 717, pp. 137222. DOI: https://doi.org/10.1016/j.scitotenv.2020.137222
2. Wang, B.; Gao, B.; Zimmerman, A.R.; Lee, X. Impregnation of multiwall carbon nanotubes in alginate beads dramatically enhances their adsorptive ability to aqueous methylene blue. Chemical Engineering Research and Design, 2018, 133, pp. 235-242. DOI: https://doi.org/10.1016/j.cherd.2018.03.026
3. Wang, Z.; Gao, M.; Li, X.; Ning, J.; Zhou, Z.; Li, G. Efficient adsorption of methylene blue from aqueous solution by graphene oxide modified persimmon tannins. Materials Science and Engineering: C, 2020, 108, 110196. DOI: https://doi.org/10.1016/j.msec.2019.110196
4. Khanday, W.A.; Asif, M.; Hameed, B.H. Cross-linked beads of activated oil palm ash zeolite/chitosan composite as a bio-adsorbent for the removal of methylene blue and acid blue 29 dyes. International Journal of Biological Macromolecules, 2017, 95, pp. 895-902. DOI: https://doi.org/10.1016/j.ijbiomac.2016.10.075
5. Makhado, E.; Pandey, S.; Ramontja, J. Microwave assisted synthesis of xanthan gum-cl-poly (acrylic acid) based-reduced graphene oxide hydrogel composite for adsorption of methylene blue and methyl violet from aqueous solution. International Journal of Biological Macromolecules, 2018, 119, pp. 255-269. DOI: https://doi.org/10.1016/j.ijbiomac.2018.07.104
6. Albayati, T.M.; Sabri, A.A.; Alazawi, R.A. Separation of methylene blue as a pollutant of water by SBA-15 in a fixed-bed column. Arabian Journal for Science and Engineering, 2016, 41, pp. 2409-2415. DOI: https://doi.org/10.1007/s13369-015-1867-7
7. Marrakchi, F.; Auta, M.; Khanday, W.A.; Hameed, B.H. High-surface-area and nitrogen-rich mesoporous carbon material from fishery waste for effective adsorption of methylene blue. Powder Technology, 2017, 321, pp. 428-434. DOI: https://doi.org/10.1016/j.powtec.2017.08.023
8. Sandoval, A.; Hernández-Ventura, C.; Klimova, T.E. Titanate nanotubes for removal of methylene blue dye by combined adsorption and photocatalysis. Fuel, 2017, 198, pp. 22-30. DOI: https://doi.org/10.1016/j.fuel.2016.11.007
9. Nguyen, C.H.; Juang, R.S. Efficient removal of methylene blue dye by a hybrid adsorption–photocatalysis process using reduced graphene oxide/titanate nanotube composites for water reuse. Journal of Industrial and Engineering Chemistry, 2019, 76, pp. 296-309. DOI: https://doi.org/10.1016/j.jiec.2019.03.054
10. Li, Q.; Li, Y,; Ma, X,; Du, Q.; Sui, K.; Wang, D.; Wang, C.; Li, H.; Xia, Y. Filtration and adsorption properties of porous calcium alginate membrane for methylene blue removal from water. Chemical Engineering Journal, 2017, 316, pp. 623-630. DOI: https://doi.org/10.1016/j.cej.2017.01.098
11. Zhang, Y.; Liu, J.; Du, X.; Shao, W. Preparation of reusable glass hollow fiber membranes and methylene blue adsorption. Journal of the European Ceramic Society, 2019, 39(15), pp. 4891-4900. DOI: https://doi.org/10.1016/j.jeurceramsoc.2019.06.038
12. Zhao, R.; Li, Y.; Sun, B.; Chao, S.; Li, X.; Wang, C.; Zhu, G. Highly flexible magnesium silicate nanofibrous membranes for effective removal of methylene blue from aqueous solution. Chemical Engineering Journal, 2019, 359, pp. 1603-1616. DOI: https://doi.org/10.1016/j.cej.2018.11.011
13. Valdés, H.; Tardón, R.F.; Zaror, C.A.; Role of surface hydroxyl groups of acid-treated natural zeolite on the heterogeneous catalytic ozonation of

methylene blue contaminated waters. Chemical Engineering Journal, 2012, 211-212, pp. 388-395. DOI: https://doi.org/10.1016/j.cej.2012.09.069

14. Kong, L.; Diao, Z.; Chang, X.; Xiong, Y.; Chen, D. Synthesis of recoverable and reusable granular MgO-SC_{CA-Zn} hybrid ozonation catalyst for degradation of methylene blue. Journal of Environmental Chemical Engineering, 2016, 4(4A), pp. 4385–4391. DOI: https://doi.org/10.1016/j.jece.2016.10.002
15. Aziz, K.H.H.; Mahyar, A.; Miessner, H.; Mueller, S.; Kalass, D.; Moeller, D.; Khorshid, I.; Rashid, M.A.M. Application of a planar falling film reactor for decomposition and mineralization of methylene blue in the aqueous media via ozonation, Fenton, photocatalysis and non-thermal plasma: A comparative study. Process Safety and Environmental Protection, 2018, 113, pp. 319-329. DOI: https://doi.org/10.1016/j.psep.2017.11.005
16. Güzel, F.; Sayğılı, H.; Akkaya Sayğılı, G.; Koyuncu, F.; Yılmaz, C. Optimal oxidation with nitric acid of biochar derived from pyrolysis of weeds and its application in removal of hazardous dye methylene blue from aqueous solution. Journal of Cleaner Production, 2017, 144, pp. 260-265. DOI: https://doi.org/10.1016/j.jclepro.2017.01.029
17. Anushree, C.; Philip, J. Efficient removal of methylene blue dye using cellulose capped Fe_3O_4 nanofluids prepared using oxidation-precipitation method. Colloids and Surfaces A, 2019, 567, pp. 193-204. DOI: https://doi.org/10.1016/j.colsurfa.2019.01.057
18. De Carvalho, H.P.; Huang, J.; Zhao, M.; Liu, G.; Dong, L.; Liu, X. Improvement of methylene blue removal by electrocoagulation/banana peel adsorption coupling in a batch system. Alexandria Engineering Journal, 2015, 54(3), pp. 777-786. DOI: https://doi.org/10.1016/j.aej.2015.04.003
19. Nippatla, N.; Philip, L. Electrocoagulation-floatation assisted pulsed power plasma technology for the complete mineralization of potentially toxic dyes and real textile wastewater. Process Safety and Environmental Protection, 2019, 125, pp. 143-156. DOI: https://doi.org/10.1016/j.psep.2019.03.012
20. Sebeia, N.; Jabli, M.; Ghith, A.; El-Ghoul, Y.; Alminderej, F.M. *Populus tremula*, *Nerium oleander* and *Pergularia tomentosa* seed fibers as sources of cellulose and lignin for the bio-sorption of methylene blue. International Journal of Biological Macromolecules, 2019, 121, pp. 655-665. DOI: https://doi.org/10.1016/j.ijbiomac.2018.10.070
21. Zhai, S.; Li, M.; Wang, D.; Zhang, L.; Yang, Y.; Fu, S. In situ loading metal oxide particles on bio-chars: Reusable materials for efficient removal of methylene blue from wastewater. Journal of Cleaner Production, 2019, 220, pp. 460-474. DOI: https://doi.org/10.1016/j.jclepro.2019.02.152
22. Abdelrahman, E.A.; Hegazey, R.M.; El-Azabawy, R.E. Efficient removal of methylene blue dye from aqueous media using Fe/Si, Cr/Si, Ni/Si, and Zn/Si amorphous novel adsorbents. Journal of Materials Research and Technology, 2019, 8(6), pp. 5301-5313. DOI: https://doi.org/10.1016/j.jmrt.2019.08.051
23. Garcia, B.B.; Lourinho, G.; Romano, P.; Brito, P.S.D. Photocatalytic degradation of swine wastewater on aqueous TiO_2 suspensions: optimization and modeling via Box-Behnken design. Heliyon, 2020, 6(1), e03293, pp. 1-8. DOI: https://doi.org/10.1016/j.heliyon.2020.e03293
24. Fouda, A.; Salem, S.S.; Wassel, A.R.; Hamza, M.F.; Shaheen, Th.I. Optimization of green biosynthesized visible light active CuO/ZnO nano-photocatalysts for the degradation of organic methylene blue dye. Heliyon, 2020, 6(9), e04896, pp. 1-13. DOI: https://doi.org/10.1016/j.heliyon.2020.e04896
25. Subramanian, Y.; Ramasamy, V.; Karthikeyan, R.J.; Srinivasan, G.R.; Arulmozhi, D.; Gubendiran, R.K.; Sriramalu, M. Investigations on the enhanced dye degradation activity of heterogeneous $BiFeO_3$–$GdFeO_3$ nanocomposite photocatalyst. Heliyon, 2019, 5(6), e01831, pp. 1-10. DOI: https://doi.org/10.1016/j.heliyon.2019.e01831
26. Mohammed, S.A.; Al-Amouri, L.; Yousif, E.; Abd-Ali, A.; Mabood, F.; Abbas, H.F.; Alyaqoobi, S. Synthesis of NiO:V_2O_5 nanocomposite and its photocatalytic efficiency for methyl orange degradation. Heliyon, 2018, 4(3), e00581, pp. 1-12. DOI: https://doi.org/10.1016/j.heliyon.2018.e00581
27. Mishra, A.; Panigrahi, A.; Mal, P.; Penta, S.; Padmaja, G.; Bera, G.; Das, P.; Rambabu, P.; Turpu, G.R. Rapid photodegradation of methylene blue dye by rGO- V_2O_5 nano composite. Journal of Alloys and Compounds, 2020, 842, pp. 155746. DOI: https://doi.org/10.1016/j.jallcom.2020.155746
28. Jayaraj, S.K.; Sadishkumar, V.; Arun, T.; Thangadurai, P. Enhanced photocatalytic activity of V_2O_5 nanorods for the photodegradation of organic dyes: A detailed understanding of the mechanism and their antibacterial activity. Materials Science in Semiconductor Processing, 2018, 85, pp. 122-133. DOI: https://doi.org/10.1016/j.mssp.2018.06.006
29. Rasheed, R.T.; Mansoor, H.S.; Al-Shaikhly, R.R.; Abdullah, T.A.; Salman, A.D.; Juzsakova, T. Synthesis and catalytic activity studies of α-MnO_2 nanorodes, rutile TiO_2 and its composite prepared by hydrothermal method. AIP Conference Proceedings, 2020, 2213(1), pp. 020122. DOI: https://doi.org/10.1063/5.0000228
30. Salman, A.D.; Juzsakova, T.; Al-Mayyahi, M.A.; Ibrahim, R.I.; Abdullah, T.A.; Khader, E.H. Improvement of mechanical properties of Oil well cement by incorporate Nano-$CaCO_3$ prepared from eggshell waste. IOP Conference Series: Material Science and Engineering, 2020, 765, 012006, pp. 1-17. DOI: https://doi:10.1088/1757-899X/765/1/012006

31. Rasheed, R.T.; Mansoor, H.S.; Abdullah, T.A.; Juzsakova, T.; Al-Jammal, N.; Salman, A.D.; Al-Shaikhly, R.; Le, P.C.; Domokos, E.; Abdulla, T.A. Synthesis, characterization of V_2O_5 nanoparticles and determination of catalase mimetic activity by new colorimetric method. Journal of Thermal Analysis and Calorimetry, 2021, 145, pp. 297-307. DOI: https://doi.org/10.1007/s10973-020-09725-5
32. Abdullah, T.A., Rasheed, R.T., Juzsakova, T.; Al-Jammal, N.; Mallah, M.A.; Cuong, L.P.; Salman, A.D.; Domokos, E.; Ali, Z.; Cretescu, I. Preparation and characterization of MnO_2-based nanoparticles at different annealing temperatures and their application in dye removal from water. International Journal Environmental Science Technology, 2021, 18, pp. 1499-1512. DOI: https://doi.org/10.1007/s13762-020-02956-x
33. Mundhe, K.S.; Gaikwad, A.B.; Torane, R.C.; Deshpande, N.R.; Kashalkar, R.V. Adsorption of methylene blue from aqueous solution using *Polyalthia longifolia* (Ashoka) seed powder. Journal of Chemical and Pharmaceutical Research, 2012, 4(1), pp. 423-436. https://www.jocpr.com/archive/jocpr-volume-4-issue-1-year-2012.html
34. Al-Jammal, N.; Abdullah, T.A.; Juzsakova, T.; Zsirka, B.; Cretescu, I.; Vágvölgyi, V.; Sebestyen, V.; Le, P.C.; Rasheed, R.T.; Domokos, E. Functionalized carbon nanotubes for hydrocarbon removal from water. Journal of Environmental and Chemical Engineering, 2020, 8(2), pp. 103570. DOI: https://doi.org/10.1016/j.jece.2019.103570
35. Wang, L.; Li, H.Y.; Wei, C.; Wang, Y.; Xie, B. Sol-Gel/Hydrothermal method for the synthesis of ultralong $(NH_4)_2V_6O_{16}\cdot 1.5H_2O$ nanobelts. In The Minerals, Metals & Materials Society (Ed.), TMS 2015 144th Annual Meeting & Exhibition, Springer: Cham, 2015, pp. 153-160. DOI: https://doi.org/10.1007/978-3-319-48127-2_20
36. Nalini, S.; Selvakumar, B.; Periasamy, P. Simple synthesis and characterization of V_2O_5 nanoparticles by microwave assisted wet chemical method. International Journal of Engineering and Manufacturing Science, 2017, 7(2), pp. 411-417. https://www.ripublication.com/Volume/ijemsv7n2.htm
37. Jadhav, C.D.; Pandit, B.; Karade, S.S.; Sankapal, B.R.; Chavan, P.G. Enhanced field emission properties of V2O5/MWCNTs nanocomposite. Applied Physics A, 2018, 124, pp. 794-802. DOI: https://doi.org/10.1007/s00339-018-2218-9
38. Sun, L.; Wan, S.; Luo, W. Biochars prepared from anaerobic digestion residue, palm bark, and eucalyptus for adsorption of cationic methylene blue dye: Characterization, equilibrium, and kinetic studies. Bioresource Technology, 2013, 140, pp. 406-413. DOI: https://doi.org/10.1016/j.biortech.2013.04.116
39. Souza, A.G.; Ferreira, O.P.; Santos, E.J.G.; Mendes, J.; Alves, O.L. Raman spectra in vanadate nanotubes revisited. Nano Letters, 2004, 4(11), pp. 2099-2104. DOI: https://doi.org/10.1021/nl0488477
40. Biedunkiewicz, A.; Gabriel, U.; Figiel, P.; Sabara, M. Investigations on NH_4VO_3 thermal decomposition in dry air. Journal of Thermal Analysis and Calorimetry, 2012, 108, pp. 965-970. DOI: https://doi.org/10.1007/s10973-011-2149-6
41. Chandar, K.N.; Jayavel, R. C_{14}TAB-assisted CeO_2 mesocrystals: self-assembly mechanism and its characterization. Applied Nanoscience, 2013, 3(3), pp. 263-269. DOI: https://doi.org/10.1007/s13204-012-0131-7
42. Wanchanthuek, R.; Thapol, A. The kinetic study of methylene blue adsorption over MgO from PVA template preparation. Journal of Environmental Science and Tehnology, 2011, 4(5), pp. 552-559. DOI: https://dx.doi.org/10.3923/jest.2011.552.559
43. Qu, S.; Huang, F.; Yu, F.; Chen, J.; Kong, J. Magnetic removal of dyes from aqueous solution using multi-walled carbon nanotubes filled with Fe_2O_3 particles. Journal of Hazardous Materials, 2008, 160(2-3), pp. 643-647. DOI: https://doi.org/10.1016/j.jhazmat.2008.03.037
44. Namasivayam, C.; Arasi, D.J.S.E. Removal of Congo red from wastewater by adsorption onto waste red mud. Chemosphere, 1997, 34(2), pp. 401-417. DOI: https://doi.org/10.1016/S0045-6535(96)00385-2
45. Zhang, Y.; Shi, R.; Yang, P.; Song, X.; Zhu, Y.; Ma, Q. Fabrication of electronspun porous CeO_2 nanofibers with large surface area for pollutants removal. Ceramics International, 2016, 42(12), pp. 14028-14035. DOI: https://doi.org/10.1016/j.ceramint.2016.06.009
46. Li, H.; Wang, G.; Zhang, F.; Cai, Y.; Wang, Y.; Djerdj, I. Surfactant-assisted synthesis of CeO_2 nanoparticles and their application in wastewater treatment. RSC Advances, 2012, 2(32), pp. 12413-12423. DOI: https://doi.org/10.1039/C2RA21590J
47. Wang, S.; Boyjoo, Y.; Choueib, A. A comparative study of dye removal using fly ash treated by different methods. Chemosphere, 2005, 60(10), pp. 1401-1407. DOI: https://doi.org/10.1016/j.chemosphere.2005.01.091
48. Ozdemir, F.A.; Demirata, B.; Apak, R. Adsorptive removal of methylene blue from simulated dyeing wastewater with melamine-formaldehyde-urea resin. Journal of Applied Polymer Science, 2009, 112(6), pp. 3442-3448. DOI: https://doi.org/10.1002/app.29835
49. Zhou, Q.; Gao, Q.; Luo, W.; Yan, C.; Ji, Z.; Duan, P. One-step synthesis of amino-functionalized attapulgite clay nanoparticles adsorbent by hydrothermal carbonization of chitosan for removal of methylene blue from wastewater. Colloids and Surfaces A, 2015, 470, pp. 248-257. DOI: https://doi.org/10.1016/j.colsurfa.2015.01.092

50. Farghali, A.A.; Bahgat, M.; El-Rouby, W.M.A.; Khedr, M.H. Decoration of MWCNTs with $CoFe_2O_4$ nanoparticles for methylene blue dye adsorption. Journal of Solution Chemistry, 2012, 41, pp. 2209-2225. DOI: https://doi.org/10.1007/s10953-012-9934-0
51. Monvisade, P.; Siriphannon, P. Chitosan intercalated montmorillonite: Preparation, characterization and cationic dye adsorption. Applied Clay Science, 2009, 42(3-4), pp. 427-431. DOI: https://doi.org/10.1016/j.clay.2008.04.013
52. Yao, Y.; Miao, S.; Liu, S.; Ma, L.P.; Sun, H.; Wang, S. Synthesis, characterization, and adsorption properties of magnetic Fe_3O_4 @ graphene nanocomposite. Chemical Engineering Journal, 2012, 184, pp. 326-332. DOI: https://doi.org/10.1016/j.cej.2011.12.017
53. Ayad, M.M.; El-Nasr, A.A.; Adsorption of cationic dye (methylene blue) from water using polyaniline nanotubes base. The Journal of Physical Chemistry C, 2010, 114(34), pp. 14377-14383. DOI: https://doi.org/10.1021/jp103780w
54. Rusu, L.; Harja, M.; Simion, A.I.; Suteu, D.; Ciobanu, G.; Favier, L. Removal of astrazone blue from aqueous solutions onto brown peat. Equilibrium and kinetics studies. Korean Journal of Chemical Engineering, 2014, 31, pp. 1008-1015. DOI: https://doi.org/10.1007/s11814-014-0009-3
55. Cho, D.-W.; Jeon, B.-H.; Chon, C.-M.; Schwartz, F.W.; Jeong, Y.; Song, H. Magnetic chitosan composite for adsorption of cationic and anionic dyes in aqueous solution. Journal of Industrial and Engineering Chemistry, 2015, 28, pp. 60-66. DOI: https://doi.org/10.1016/j.jiec.2015.01.023
56. Harja, M.; Barbuta, M.; Rusu, L.; Munteanu, C.; Buema, G.; Doniga, E. Simultaneous removal of astrazone blue and lead onto low cost adsorbents based on power plant ash. Environemntal Engineering and Management Journal, 2011, 10(3), pp. 341-347. DOI: 10.30638/eemj.2011.050
57. Ahmadi, S.; Igwegbe, C.A. Removal of methylene blue on zinc oxide nanoparticles: Nonlinear and linear adsorption isotherms and kinetics study. Sigma Journal of Engineering and Natural Science, 2020, 38(1), pp. 289-303. https://eds.yildiz.edu.tr/sigma/Articles
58. de Castro, M.L.F.A.; Abad, M.L.B.; Sumalinog, D.A.G.; Abarca, R.R.M.; Paoprasert, P.; de Luna, M.D.G. Adsorption of methylene blue dye and Cu(II) ions on EDTA-modified bentonite: isotherm, kinetic and thermodynamic studies. Sustainable Environment Research, 2018, 28(5), pp. 197-205. DOI: https://doi.org/10.1016/j.serj.2018.04.001
59. Zhou, T.; Lu, W.; Liu, L.; Zhu, H.; Jiao, Y.; Zhang, S.; Han, R. Effective adsorption of light green anionic dye from solution by CPB modified peanut in column mode. Journal of Molecular Liquids, 2015, 211, pp. 909-914. DOI: https://doi.org/10.1016/j.molliq.2015.08.018
60. Kajjumba, G.W.; Emik, S.; Ongen, A.; Ozcan, H.K.; Aydin, S. Modelling of adsorption kinetic processes—Errors, Theory and Application. IntechOpen: Rijeka, 2019, pp. 1-19. DOI: https://doi.org/10.5772/intechopen.80495
61. Somsesta, N.; Sricharoenchaikul, V.; Aht-Ong, D. Adsorption removal of methylene blue onto activated carbon/cellulose biocomposite films: Equilibrium and kinetic studies. Materials Chemistry and Physics, 2020, 240, 122221. DOI: https://doi.org/10.1016/j.matchemphys.2019.122221
62. Tuli, F.J.; Hossain, A.; Kibria, A.K.M.F.; Tareq, A.R.M.; Mamun, S.M.M.A.; Ullah, A.K.M.A. Removal of methylene blue from water by low-cost activated carbon prepared from tea waste: A study of adsorption isotherm and kinetics. Environmental Nanotechnology, Monitoring and Management, 2020, 14, 100354. DOI: https://doi.org/10.1016/j.enmm.2020.100354
63. Tran, T.H.; Le, A.H.; Pham, T.H.; Nguyen, D.T.; Chang, S.W.; Chung, W.J.; Nguyen, D.D. Adsorption isotherms and kinetic modeling of methylene blue dye onto a carbonaceous hydrochar adsorbent derived from coffee husk waste. Science of The Total Environment, 2020, 725, 138325. DOI: https://doi.org/10.1016/j.scitotenv.2020.138325